ELSEVIER

Available online at www.sciencedirect.com

SCIENCE DIRECT®

Journal of Solid State Chemistry 179 (2006) 1009–1015

JOURNAL OF SOLID STATE CHEMISTRY

www.elsevier.com/locate/jssc

NMR study of the order–disorder phase transitions of $KHCO_3$ and $KDCO_3$ single crystals

Ae Ran Lim[a,*], Se-Young Jeong[b]

[a]Department of Science Education, Jeonju University, Jeonju 560-759, Korea
[b]School of Nanoscience & Technology, Pusan National University, Pusan 609-735, Korea

Received 19 September 2005; received in revised form 14 December 2005; accepted 16 December 2005

Abstract

$KHCO_3$ and its deuterated analogue $KDCO_3$ are typical materials that undergo order–disorder phase transitions at 318 and 353 K, respectively. The spin–lattice relaxation times, T_1, spin–spin relaxation times, T_2, and the number of resonance lines for the ^1H, ^2D, and ^{39}K nuclei of these crystals were investigated using NMR spectrometer. These materials are known to exhibit anomalous decreases in T_1 near T_C, which have been attributed to a structural phase transition. Additionally, changes in the symmetry of the $(HCO_3)_2^{2-}$ (or $(DCO_3)_2^{2-}$) dimers in these materials are associated with large changes in T_1, T_2, and the number of resonance lines. Here we found that the resonance lines for ^1H, ^2D, and ^{39}K nuclei decrease in number as the temperature is increased up to T_C, indicating that the orientations of the $(HCO_3)_2^{2-}$ (or $(DCO_3)_2^{2-}$) dimers and the environments of the K ions change at T_C. Moreover, based on number of resonance lines, the results further indicate that the $(HCO_3)_2^{2-}$ (or $(DCO_3)_2^{2-}$) dimers reorientate to approximately parallel to the directions of the hydrogen bonds (or deuteron bonds) and the direction of the *a*-axis. The transitions at 318 and 345 K of the two crystals are of the order–disorder type. The present results therefore indicate that the orientations of the $(HCO_3)_2^{2-}$ and $(DCO_3)_2^{2-}$ dimers and the environment of the K ion play a significant role in these phase transitions.

Keywords: Physics of crystal growth; Disordered solids; Nuclear magnetic resonance and relaxation; Phase transition

1. Introduction

Potassium bicarbonate, $KHCO_3$, belongs to the class of materials that are composed of hydrogen-bonded dimers. These systems provide tools for investigating the properties of hydrogen bonding, which plays an important role in various aspects of the natural sciences, including the life sciences [1]. There has also been considerable interest in the order–disorder phase transitions of these materials. $KHCO_3$ and its deuterated analogue $KDCO_3$ are typical of materials that exhibit order–disorder phase transitions. They undergo antiferrodistortive phase transitions of order–disorder type at T_C, which is at 318 K for $KHCO_3$ and at 353 K for $KDCO_3$ [2–5]. Note the significant isotope effect on the transition temperature. The low- and high-temperature phases of these materials have been shown to have monoclinic structures with space group $P2_1/a$ and monoclinic structures with space group $C2/m$ respectively [2,3,6–9]. Pairs of HCO_3 (or DCO_3) molecules are linked by two hydrogen (or deuteron) bonds in a plane, forming a $(HCO_3)_2^{2-}$ (or $(DCO_3)_2^{2-}$) dimer [2,10–12]. Haussuhl [13] reported that the orientation of the $(HCO_3)_2^{2-}$ dimer plays a large role in the order–disorder phase transition of $KHCO_3$.

The $(HCO_3)_2^{2-}$ and $(DCO_3)_2^{2-}$ dimers in $KHCO_3$ and $KDCO_3$ single crystals are partially disordered at room temperature because of the two equilibrium positions of hydrogen and deuterium. According to Kashida and Yamamoto [2], the hydrogens occupy the two equilibrium positions with half occupancies in the high-temperature phase, whereas in the low-temperature phase they are almost localized at one site; they concluded that the phase transition can be described in terms of the order–disorder

---

*Corresponding author. Fax: +82 063 220 2054.
E-mail addresses: aeranlim@hanmail.net, arlim@jj.ac.kr (A.R. Lim).

0022-4596/$ - see front matter © 2005 Elsevier Inc. All rights reserved.
doi:10.1016/j.jssc.2005.12.029

of the $(HCO_3)_2^{2-}$ dimers. Nuclear magnetic resonance (NMR) studies of some of the physical properties of $KHCO_3$ and $KDCO_3$ have been carried out by several investigators. Deuteron NMR was carried out for this system by Chiba [14] and Poplett et al. [15], who determined the quadrupole parameter at room temperature. Feucht et al. [16] determined the proton-shielding tensors of these materials using NMR. These results indicate the degree of ionization of the protons in the hydrogen bonds. In addition, the mechanism of proton transfer in the dimer has been studied with ^{17}O quadrupole double resonance [9,17]. Benz et al. [18] measured the orientation and temperature dependences of spin–lattice relaxation time for the deuterons in $KDCO_3$ below T_C, and discussed the jump motions of deuterons along the hydrogen bonds. Also, we have previously reported the ^1H and ^{39}K spin–lattice relaxation times in $KHCO_3$ crystals. The changes in the relaxation time near T_C ($= 318\,K$) indicates that the ^1H and ^{39}K ions were significantly affected during this transition. And, the ^{39}K spin–lattice relaxation time was in accordance with the Raman process below and above T_C [19]. Recently, Odin [20] investigated the phase transition of powder $KHCO_3$ by the ^{13}C and ^{39}K high-resolution solid-state NMR. This result appeared that the anisotropy and asymmetry parameters of the carbon chemical shift and potassium quadrupolar interaction tensors are strongly affected by the phase transition.

The association of the dynamical transfer of hydrogen atoms with structural phase transitions has been the subject of keen interest. In this connection, the protons and deuterons of $KHCO_3$ and $KDCO_3$ single crystals are particularly worthy of study. In the present study, we investigated the temperature dependences of the spin–lattice relaxation time, T_1, and the spin–spin relaxation time, T_2, of the ^1H, ^2D, and ^{39}K nuclei in $KHCO_3$ and $KDCO_3$ single crystals in order to elucidate the mechanisms of their structural phase transitions, with particular emphasis on the role within those mechanisms of hydrogen bonding. Our observations of the relaxation times of ^1H, ^2D, and ^{39}K nuclei in $KHCO_3$ and $KDCO_3$ single crystals are new results.

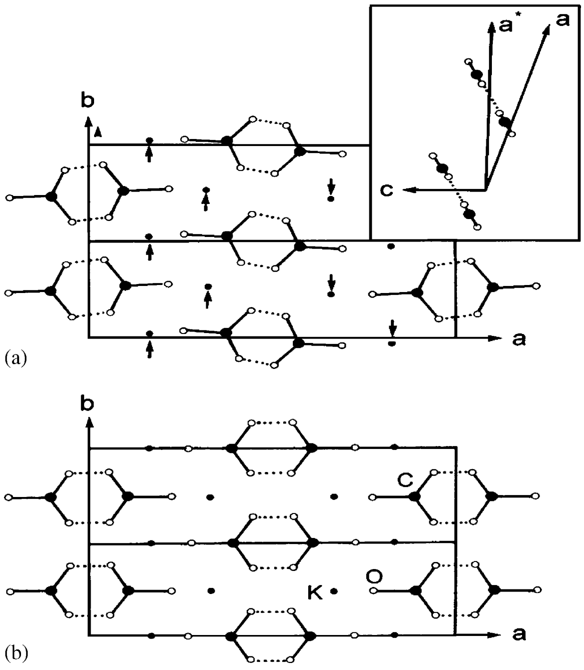

Fig. 1. Schematic drawing of the $KHCO_3$ crystal structure projected onto the *ab*-plane (a) for the low-temperature phase belonging to the space group $P2_1/a$ (inset: projection along the *b*-axis) and (b) for the high-temperature phase belonging to the space group $C2/m$. The hydrogen bonds are represented by dotted lines. The arrows represent displacement from the symmetrical positions occupied in the high-temperature phase.

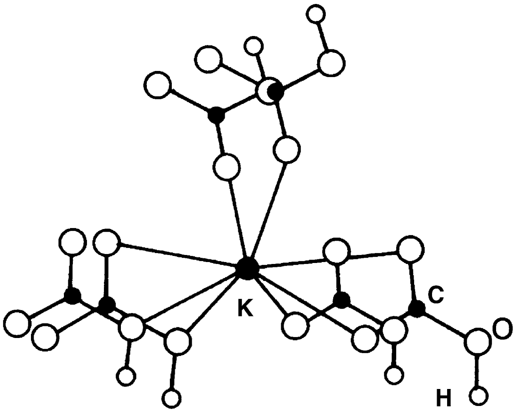

Fig. 2. The environment of the K^+ ion in $KHCO_3$ at 298 K.

2. Crystal structure

Single crystals of $KHCO_3$ are monoclinic with space group $P2_1/a$, with cell parameters $a = 15.1725\,Å$, $b = 5.6283\,Å$, $c = 3.7110\,Å$, and $\beta = 104.631°$; there are $Z = 4$ molecules in the unit cell at 298 K [7,8]. The HCO_3^- anion dimers are linked by two adjacent hydrogen bonds. These centrosymmetric dimers $(HCO_3)_2^{2-}$ have relatively strong $O\text{–}H\cdots O$ hydrogen bonds. The two protons of each dimer are related by a center of symmetry, as shown in Fig. 1(a), and are therefore magnetically equivalent. The two hydrogen bonds within each dimer are symmetrically equivalent through an inversion operation. At high temperatures, the crystals are monoclinic with space group $C2/m$ ($Z = 4$), with cell parameters $a = 15.195\,Å$, $b = 5.640\,Å$, $c = 3.734\,Å$, and $\beta = 104.86°$ at 353 K. The projection of the structure in the high temperature phase onto the *ab*-plane is shown in Fig. 1(b). Each K^+ ion has eight neighboring oxygen atoms, as shown in Fig. 2. The average bond lengths for K–O below and above T_C are 2.843 Å and 2.854 Å, respectively.

Potassium deuterium carbonate, $KDCO_3$, is monoclinic with space group $P2_1/a$ with cell parameters $a = 15.1948\,Å$, $b = 5.6307\,Å$, $c = 3.7107\,Å$, and $\beta = 104.567°$ at room temperature [7,8]. Above T_C, the structure is monoclinic with space group $C2/m$. This structure is very similar to the $KHCO_3$ structure shown in Fig. 1.

3. Experimental procedure

The $KHCO_3$ and $KDCO_3$ single crystals were obtained by slow recrystallization from aqueous solution in H_2O and D_2O, respectively. Colorless prismatic crystals elongated along the *c*-axis were generally formed on cooling.

The spin–lattice and spin–spin relaxation times of the ^{1}H, ^{2}D, and ^{39}K nuclei in $KHCO_3$ and $KDCO_3$ single crystals were measured using the Bruker MSL 200 FT NMR and Bruker DSX 400 FT NMR spectrometers at the Korea Basic Science Institute. The static magnetic fields we used were 4.7 and 9.4 T, respectively, and the central radio frequencies were set at $\omega_0/2\pi = 200$ MHz for the ^{1}H nucleus, $\omega_0/2\pi = 61.40$ MHz for the ^{2}D nucleus, and at $\omega_0/2\pi = 18.672$ MHz for the ^{39}K nucleus. The spin–lattice relaxation times were measured by applying a pulse sequence of π–t–$\pi/2$. The nuclear magnetizations $S(t)$ of the ^{1}H, ^{2}D, and ^{39}K nuclei at time t after the π pulse were determined from the inversion recovery sequence following the pulse. The width of the π pulse was 5 μs for ^{1}H, 5 μs for ^{2}D, and 33.3 μs for ^{39}K, respectively. The spin–spin relaxation time, T_2, measured with the solid echo method by applying a $\pi/2$–t–$\pi/2$ pulse sequence. The temperature dependences of the NMR measurements were obtained in the temperature range 150–410 K. Each sample temperature was held constant by controlling the nitrogen gas flow and heater current, giving an accuracy of ±0.5 K.

4. Experimental results and analysis

The ^{1}H, ^{2}D, and ^{39}K spin–lattice relaxation times were obtained for the $KHCO_3$ and $KDCO_3$ single crystals. The recovery traces of the ^{1}H ($I = 1/2$) nuclei follow a single exponential function. Thus, the spin–lattice relaxation time was determined by fitting it with the recovery pattern given by the following equation [21,22]:

$$M(\infty) - M(t) = 2M(\infty)\exp(-Wt), \tag{1}$$

where $M(t)$ is the nuclear magnetization at time t, and W is the transition probability corresponding to $\Delta m = \pm 1$. The relaxation times are given by

$$T_1 = 1/W. \tag{2}$$

The recovery traces for the central line of ^{39}K ($I = 3/2$) with dominant quadrupole relaxation can be represented by a linear combination of two exponential functions, as in Eq. (3) [23]:

$$M(\infty) - M(t) = 2M(\infty)[0.5\exp(-2W_1 t) + 0.5\exp(-2W_2 t)], \tag{3}$$

where W_1 and W_2 are the transition probabilities for $\Delta m = \pm 1$ and $\Delta m = \pm 2$, respectively. Thus, the relaxation times are given by

$$1/T_1 = 0.4(W_1 + 4W_2). \tag{4}$$

4.1. ^{1}H and ^{39}K spin–lattice relaxation times in $KHCO_3$ single crystal

As the $KHCO_3$ crystal has two orientationally inequivalent dimers, its solid state ^{1}H NMR spectrum is expected to consist of two resonance lines. The two types of dimers are related by the monoclinic glide plane, as shown in Fig. 1(a). Only one line is expected in the proton spectrum for the special case when B_o lies in the glide plane. We used single crystals oriented with respect to the direction of the *a*-axis, and two ^{1}H signal is obtained in the temperature range 150–315 K, as shown in Fig. 3. Above T_C, two resonance signals are reduced to only one resonance signal. This means that the orientations of the $(HCO_3)_2^{2-}$ dimers change at 318 K, becoming approximately parallel to the directions of the hydrogen bonds and the direction of the *a*-axis. The ^{39}K ($I = 3/2$) NMR spectrum consists of a pair of satellite lines ($m = -3/2 \leftrightarrow -1/2$) and ($m = 1/2 \leftrightarrow 3/2$), and a central line ($m = +1/2 \leftrightarrow -1/2$). Usually, the

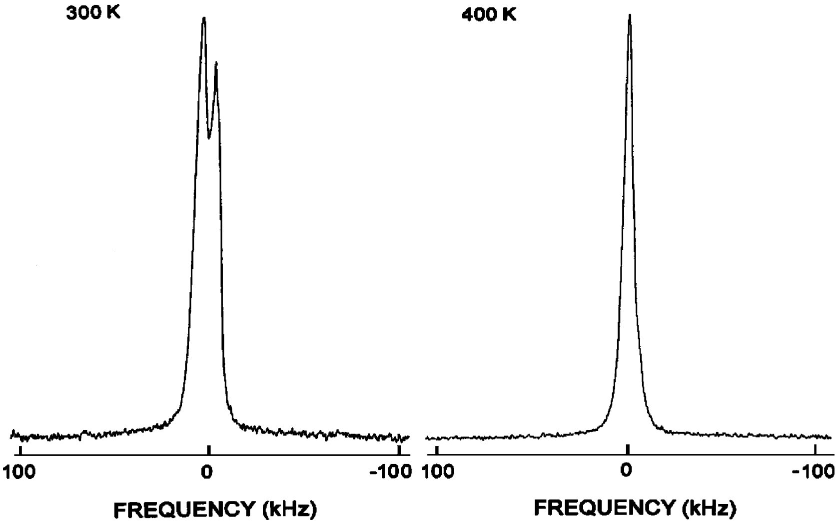

Fig. 3. ^{1}H NMR spectrum below and above T_C in $KHCO_3$ crystals.

magnitudes of the quadrupole parameters of ^{39}K nuclei are on the order of MHz. Two satellite lines for the ^{39}K nucleus are far away from the central line. Therefore, the satellite lines are not easy to obtain. From the our ^{39}K NMR result, two resonance lines are obtained in the temperature range 150–315 K instead of three resonance lines, and only one resonance line is obtained above T_C. This means that the two central resonance lines by the two orientationally inequivalent types of K ion surrounded by oxygen ions below T_C changes the one central resonance line by the orientationally equivalent type of K ion surrounded by oxygen ions at T_C.

The recovery traces of the magnetization of the crystals were measured at several temperatures, and the spin–lattice relaxation time, T_1, was obtained. The recovery traces for ^{1}H can be described with a single exponential function as in Eq. (1), whereas those for ^{39}K can be described with a linear combination of two exponential functions, such as in Eq. (3). The temperature dependences of T_1 for the ^{1}H and ^{39}K nuclei in this single crystal are shown in Fig. 4. The temperature dependences of the spin–lattice relaxation behavior of the ^{1}H and ^{39}K nuclei were found to be quite similar. The relaxation times of the ^{1}H and ^{39}K nuclei undergo significant changes near 318 K, indicating drastic alterations in spin dynamics at the transition temperature. The changes in the T_1 curves near 318 K correspond to the first-order phase transition. The spin–lattice relaxation time T_1 of ^{1}H in KHCO$_3$ was found to be long: 517 s at 230 K and 141 s at 350 K. The relaxation times of ^{39}K were found to be short: 2.40 s at 220 K and 0.32 s at 350 K. In both cases, the relaxation time was found to decrease with increases in temperature below T_C, whereas it increased with increases in temperature above T_C [19]. The relaxation time of ^{1}H was found to be longer than that of ^{39}K.

From the proton spin–lattice relaxation time T_1 measurements shown in Fig. 4, one can derive the correlation time τ_H for the reorientation of (HCO$_3$)$^-$ in KHCO$_3$. The proton relaxation is mainly controlled by the H–H intradipolar interaction modulated by (HCO$_3$)$^-$ reorientation. The temperature dependence of T_1 is described by the spectral density function [24,25]:

$$\begin{aligned} T_1^{-1} &= C(\gamma^4\hbar^2/r^6)[J(\omega_o) + 4J(2\omega_o)] \\ &= C(\gamma^4\hbar^2/r^6)[\tau_H/(1+\omega_o^2\tau_H^2) + 4\tau_H/(1+4\omega_o^2\tau_H^2)], \end{aligned} \tag{5}$$

here, C is a dimensionless constant of order unity that depends on the details of the motion, γ represents the gyromagnetic ratio for the ^{1}H nucleus, r is the proton–proton distance, $\hbar = h/2\pi$ where h is Planck's constant, and ω_o represents the proton Larmor frequency. The minima occur when the (HCO$_3$)$^-$ have $\omega_o\tau_H = 0.616$. The Bloembergen–Purcell–Pound (BPP) [26] relation between T_1 and the characteristic frequency of motion ω_o can be applied. Since the T_1 curves were found to exhibit a minimum, it was possible to determine the constant in the BPP formula. We were then able to calculate the parameter τ_H as a function of temperature. The τ_H at 250 and 380 K is 4.4×10^{-9} and 5.8×10^{-10} s, respectively.

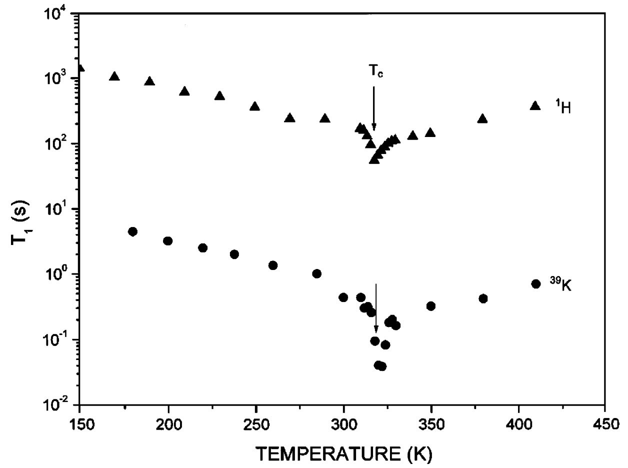

Fig. 4. Temperature dependences of the ^{1}H and ^{39}K spin–lattice relaxation times for a KHCO$_3$ single crystal.

The temperature dependence of T_1 was found to follow an Arrhenius law

$$T_1 = A \exp(-E_a/kT), \tag{6}$$

where E_a is the activation energy for reorientational motion. The activation energies for KHCO$_3$ crystals were determined by a curve fitting of Eq. (6). The E_a above and below T_C were determined to be 16.63 and 6.64 kJ/mol for the ^{1}H nucleus, respectively, and 15.35 and 6.02 kJ/mol for the ^{39}K nucleus, respectively. Above and below T_C, the activation energies for the ^{1}H nucleus are similar to those for the ^{39}K nucleus. The activation energy defined by the Arrhenius law is related to the motion of nuclei. The dipolar interaction between nuclear spins, which is modulated by motion of the nuclei, acts as a mechanism of spin–lattice relaxation for ^{1}H. In the KHCO$_3$ system, this corresponds to motion of the hydrogen atom within the hydrogen bonds; the potassium atoms are not involved in this type of dynamics. However, the spin interactions determining the spin–lattice relaxation for both ^{1}H and ^{39}K nuclei are probably coupled, which means that the dynamics of the protons influences the dipolar and quadrupolar interactions controlling the spin–lattice relaxation of ^{39}K nuclei. This may explain the similar values of the activation energy parameters determined from the experimental ^{1}H and ^{39}K NMR data. Therefore, both nuclei are significantly affected during this transition.

4.2. ^{2}D and ^{39}K spin–lattice relaxation times in KDCO$_3$ single crystal

KDCO$_3$ crystals have two orientationally inequivalent dimers, so the ^{2}D ($I = 1$) NMR spectrum is expected to consist of four lines. Four lines are expected in the deuterium spectrum when B_o does not lie in the glide plane. Four signals were obtained for the ^{2}D nuclei in KDCO$_3$ for the temperature range 160–340 K, and above 345 K, these four signals are reduced to two signals, as shown in Fig. 5. The splitting of the ^{2}D resonance lines were found to change slightly, and the spacing between the resonance lines decreases with increasing temperature, as shown in Fig. 6. The ^{2}D spectrum does change from four resonance lines to two resonance lines near 345 K. This means that the orientations of the $(DCO_3)_2^{2-}$ dimers change at 345 K, becoming approximately parallel to the directions of the deuterium bonds and the direction of the *a*-axis. The ^{39}K NMR spectrum has three resonance lines as a result of the quadrupole interactions of the ^{39}K ($I = 3/2$) nuclei. When the crystal is rotated about the crystallographic axis, crystallographically equivalent nuclei give rise to three lines: one central line and two satellite lines. Instead of three resonance lines for the ^{39}K nuclei in $KDCO_3$ crystals, two resonance lines are obtained in the temperature range 160–340 K and one resonance line is measured above T_C, as shown in Fig. 7. When B_o does not lie in the glide plane, two resonance lines are obtained by the central transition ($+1/2 \leftrightarrow -1/2$) of the ^{39}K NMR spectrum. Above 345 K, only one resonance line is obtained for K nuclei. The splitting of the ^{39}K resonance lines as a function of temperature is shown in Fig. 8. As indicated by the results for the ^{2}D nuclei, the environment of the K nuclei changes above 345 K. Further, the change in the number of resonance lines is associated with the phase transition at 345 K; the change in the symmetry of the K ion surrounded by oxygen ions plays an important role in the phase transition.

The variations with temperature of the spin–lattice and spin–spin relaxation times for the four lines of ^{2}D in $KDCO_3$ were measured. The recovery traces for the four resonance lines of ^{2}D can be represented by a single exponential function, as in Eq. (1). The ^{2}D relaxation times in $KDCO_3$ are displayed in Fig. 9. The values of T_1 for the four resonance lines below T_C are very similar, and are the same within experimental error. The values of T_1 for the two resonance lines above T_C are also very similar, and are the same within experimental error. The relaxation time for the ^{2}D nuclei undergoes a significant change near 345 K, indicating a drastic alteration of spin dynamics at the transition temperature. The decrease in T_1 near T_C is due to a structural phase transition. At all temperatures, T_1 is different from T_2. T_1 below T_C is determined by the slow $(DCO_3)^-$ rotational reorientations, whereas the T_1 above T_C is determined by the fast $(DCO_3)^-$ rotational reorientations. As the temperature increases, ω_c (reorientation) speeds up, causing a narrowing of the proton NMR linewidth and, as a result, T_2 increases near T_C. This increase

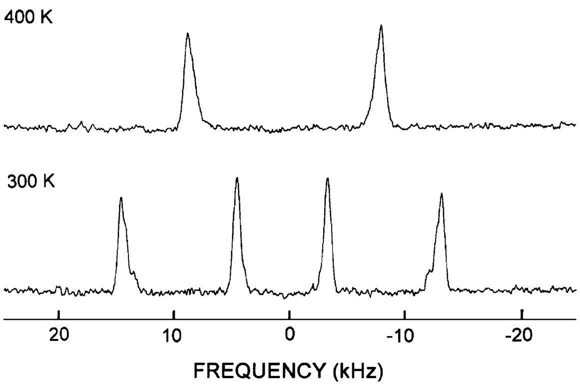

Fig. 5. ^{2}D NMR spectrum below and above T_C in $KDCO_3$ crystals.

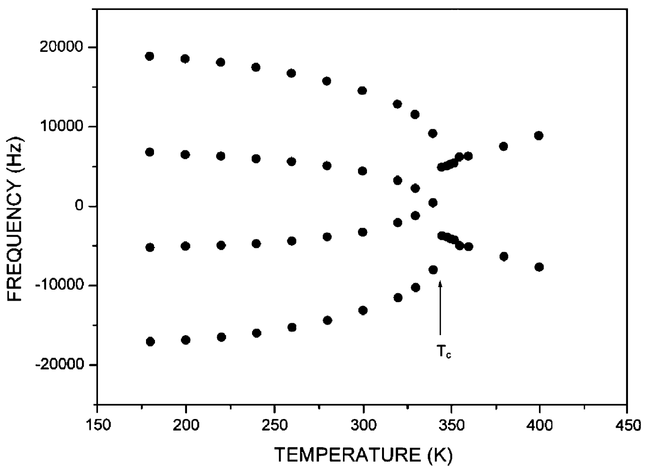

Fig. 6. Splitting of the ^{2}D resonance line as a function of temperature for $KDCO_3$.

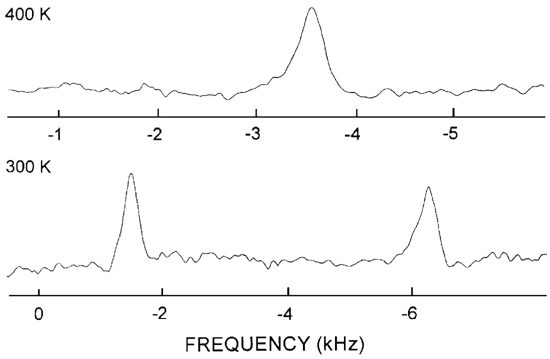

Fig. 7. ^{39}K NMR spectrum below and above T_C in $KDCO_3$ crystals.

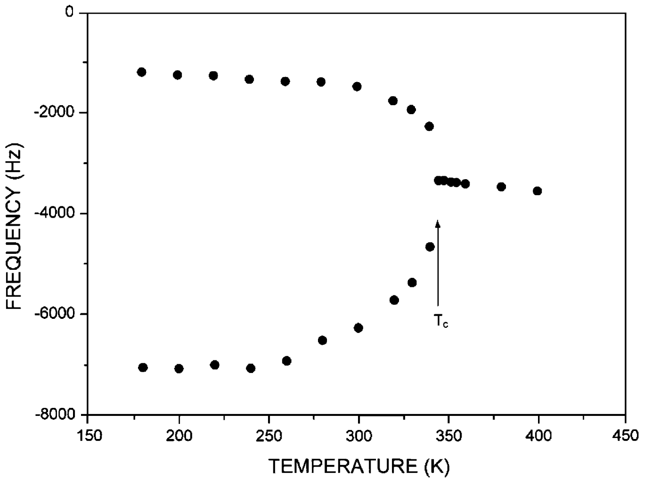

Fig. 8. Splitting of the ^{39}K resonance line as a function of temperature for $KDCO_3$.

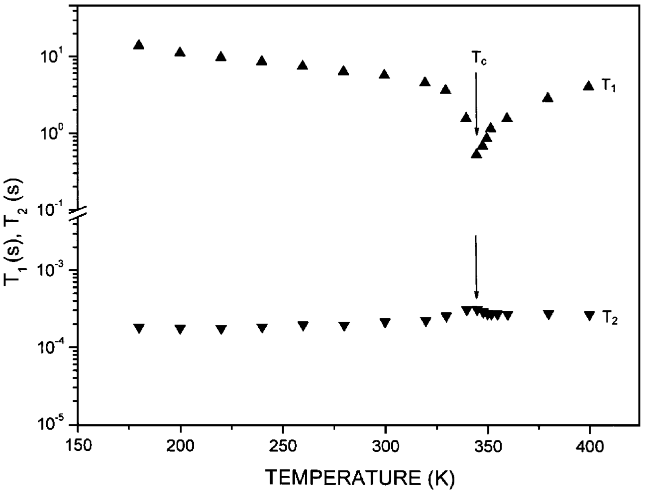

Fig. 9. Temperature dependences of T_1 and T_2 of ^{2}D in a $KDCO_3$ single crystal.

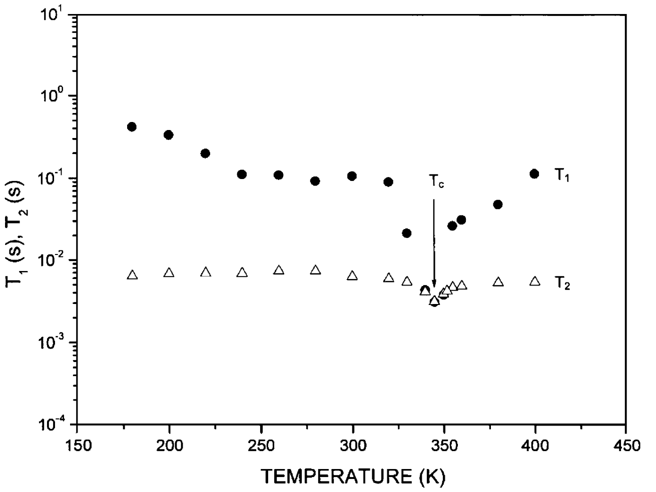

Fig. 10. Temperature dependences of T_1 and T_2 of ^{39}K in a $KDCO_3$ single crystal.

in T_2 near T_C is due to the rapid motion of the deuterium in $(DCO_3)^-$ ions. The temperature dependences of the nuclear spin–lattice relaxation times of the ^{39}K nuclei are shown in Fig. 10. The inversion recovery traces of ^{39}K can be described with a linear combination of two exponential functions. The temperature dependence of T_1 for ^{39}K is nearly the same as that of ^{2}D, undergoing a significant change near 345 K, and indicating a drastic alteration of the spin dynamics at the transition temperature, as usually occurs in a structural phase transition. T_1 for ^{39}K is less than T_1 for ^{2}D, and the ^{2}D and ^{39}K relaxation times exhibit similar temperature dependence. The ^{2}D and ^{39}K T_1 for $KDCO_3$ decrease for increases in temperature up to 320 K, and at higher temperatures the relaxation times increase with temperature.

The correlation time τ_D for the $(DCO_3)^-$ reorientation can be obtained from the ^{2}D spin–lattice relaxation data shown in Fig. 9. In this case, the relaxation is driven by the coupling of the deuteron quadrupole moment Q with the intramolecular fluctuating electric field gradient of the reorienting $(DCO_3)^-$, and T_1 is given by [24,25]

$$T_1^{-1} = C(e^2qQ/h)^2[\tau_D/(1+\omega_o^2\tau_D^2) + 4\tau_D/(1+4\omega_o^2\tau_D^2)], \tag{7}$$

where e^2qQ/h is the quadrupole coupling constant for ^{2}D. The minima occur when the $(DCO_3)^-$ have $\omega_o\tau_D = 0.616$. The τ_D at 250 and 380 K is 3.2×10^{-8} and 1.4×10^{-10} s, respectively. The activation energies obtained from the portions of the log of T_1 versus the $1000/T$ curve above and below T_C were derived to be 28.51 and 5.41 kJ/mol for ^{2}D nucleus, respectively, and 42.5 and 6.93 kJ/mol for ^{39}K nucleus, respectively. The large changes of the activation energies above and below T_C indicates that the D and K ions are significantly affected during this transition.

5. Discussion and conclusion

Information about the structure and internal motions of solids can be obtained using NMR techniques. In measurements of relaxation time as a function of temperature, it is often found that the slope of the relaxation time undergoes a change in the neighborhood of a phase transition temperature. The interest in such research lies in the associations between changes in spin–lattice relaxation times and structural phase transitions.

The spin–lattice and spin–spin relaxation times of ^{1}H, ^{2}D, and ^{39}K nuclei in $KHCO_3$ and $KDCO_3$ crystals were measured. The large changes in the relaxation times at 318 and 345 K for the two crystals indicate that the H, D, and K ions are significantly affected during this transition. This indicates that the phase I to phase II transition is first order. The relaxation time slowly decreases as the temperature is increased, whereas at high temperatures it increases with increasing temperature. This type of anomalous decrease in T_1 around T_C is usually indicative of a structural phase transition. The value of the spin–lattice relaxation time is determined by spin interaction modulated by the dynamics of the nuclei.

Our results indicate that changes in the symmetry of the dimers are associated with the large changes in the spin-lattice and spin–spin relaxation times, and in the number of resonance lines. The changes of the resonance lines for ^{1}H, ^{2}D, and ^{39}K nuclei means that the orientations of the $(HCO_3)_2^{2-}$ (or $(DCO_3)_2^{2-}$) dimers and the environments of K ions change at T_C, becoming approximately parallel to the directions of the hydrogen bonds (or deuteron bonds) and the direction of the *a*-axis. The structural phase transitions of $KHCO_3$ and $KDCO_3$ may be associated with symmetry changes of the $(HCO_3)_2^{2-}$ and $(DCO_3)_2^{2-}$ dimers and of the K ion surrounded by oxygen atoms with elevation of temperature. Therefore, the orientations of the $(HCO_3)_2^{2-}$ and $(DCO_3)_2^{2-}$ dimers and the environments of K ion play important roles in the phase transitions. In other words, the transitions at 318 and 345 K of the two crystals are of the order–disorder type. During these transitions the structure changes from that of the room-temperature phase (monoclinic, space $P2_1/a$) to that of the high-temperature phase (monoclinic, space group $C2/m$). We have investigated the isotope effect on the phase transitions of $KHCO_3$ and $KDCO_3$, and the difference of the two crystals shows the discrepancy of the transition temperature. From the NMR result, the new information can be obtained from measurements on single crystals, which is not accessible from powder data.

Poplett and Smith [15] reported the quadrupole parameters of ^{2}D in $KDCO_3$; the quadrupole coupling constant and asymmetry parameter are $e^2qQ/h = 154.7$ kHz and $\eta = 0.189$ for site 1, and $e^2qQ/h = 152.6$ kHz and $\eta = 0.193$ for site 2, respectively. However, ^{39}K NMR studies in $KHCO_3$ and $KDCO_3$ single crystals have not been reported until now. Given that no information is available on the parameters describing the quadrupole interaction of ^{39}K nuclei, the activation energies obtained from our experimental results above and below T_C cannot be compared with the quadrupole parameters of $KHCO_3$ and $KDCO_3$ crystals, respectively. On the other hand, the protons were disordered in an asymmetric double-well potential in the low-temperature phase, and the double-well potential becomes symmetric in the high-temperature phase [7,8,27,28]. Thus, the comparison between the activation energies of ^{1}H and ^{2}D in $KHCO_3$ and $KDCO_3$ crystals provides an ideal basis on which to understand relationships for molecular motion within the double-well potential. In the low-temperature phase, the dimers are tilted and the protons are distributed between the two wells of an asymmetric double-well potential. At low temperature, the motion is slow compared to the Larmor frequency and the populations of the two sites are more unequal; hence, the relaxation rate decreases with decreasing temperature, with the slope of $\log T_1^{-1}$ versus $1/T$ corresponding to the activation energy E_a. In the high-temperature phase, the dimers are not tilted and the double-well potential becomes symmetric. At high temperature, the motion is fast compared to the Larmor frequency and the populations of the two sites become more equal; hence, the relaxation rate increases with decreasing temperature, with the slope of $\log T_1^{-1}$ versus $1/T$ corresponding to the E_a for molecular motion. The values of E_a for the ^{1}H in $KHCO_3$ in the low- and high-temperature regimes are very different from the corresponding values for ^{2}D in $KDCO_3$, suggesting the presence of an isotope effect.

Acknowledgment

This work was supported by the Korea Research Foundation Grant funded by Korean Government (R04-2003-000-10040-0).

References

[1] R. Kanao, S.I. Nohdo, N. Horiuchi, S. Kashida, K. Kakurai, Y. Yamada, J. Phys. Soc. Japan 65 (1996) 1710.
[2] S. Kashida, K. Yamamoto, J. Solid State Chem. 86 (1990) 180.
[3] M. Machida, Y. Yamaguchi, M. Sugiyama, Y. Iwata, N. Koyano, S. Fukui, Physica B 213 & 214 (1995) 393.
[4] R. Kanao, S.I. Nohdo, N. Horiuchi, S. Kashida, K. Kakurai, Y. Yamada, J. Phys. Soc. Japan 64 (1995) 2286.
[5] K. Kakurai, T. Sakaguchi, M. Nishi, C.M.E. Zeyen, S. Kashida, Y. Yamada, Phys. Rev. B 53 (1996) R5974.
[6] I. Nitta, Y. Tomiie, C.H. Koo, Acta Crystallogr. 5 (1952) 292.
[7] J.O. Thomas, R. Tellgren, I. Olovsson, Acta Crystallogr. B 30 (1974) 1155.
[8] J.O. Thomas, R. Tellgren, I. Olovsson, Acta Crystallogr. B 30 (1974) 2540.
[9] J.B. Larcombe-McDouall, J.A.S. Smith, J. Chem. Soc. Faraday Trans. 2. 85 (1989) 53.
[10] F. Fillaux, Chem. Phys. 74 (1983) 405.
[11] S. Ikeda, F. Fillaux, Phys. Rev. B 59 (1999) 4134.
[12] F. Fillaux, A. Cousson, D. Keen, Phys. Rev. B 67 (2003) 054301.
[13] S. Haussuhl, Solid State Commun. 57 (1986) 643.
[14] T. Chiba, J. Chem. Phys. 41 (1964) 1352.
[15] I.J.F. Poplett, J.A.S. Smith, J. Chem. Soc., Faraday Trans. 2 74 (1978) 1077.
[16] H. Feucht, U. Haeberlen, M.P. Stachura, H.W. Spieβ, Z. Naturforsch. 31a (1976) 1173.
[17] A. Gough, M.I. Haq, J.A.S. Smith, Chem. Phys. Lett. 117 (1985) 389.
[18] S. Benz, U. Haeberlen, J. Tegenfeldt, J. Magn. Reson. 66 (1986) 125.
[19] A.R. Lim, S.Y. Jeong, Phys. Stat. Sol. (b) 226 (2001) 413.
[20] C. Odin, J. Phys. Chem. B 108 (2004) 7402.
[21] A. Abragam, The Principles of Nuclear Magnetism, Oxford University Press, Oxford, 1961.
[22] B. Cowan, Nuclear Magnetic Resonance and Relaxation, Cambridge University Press, Cambridge, 1997.
[23] M. Igarashi, H. Kitagawa, S. Takahashi, R. Yoshizak, Y. Abe, Z. Naturforsch. 47a (1992) 313.
[24] F. Borsa, R.G. Barnes, B.J. Beaudry, D.R. Torgeson, Phys. Rev. B 26 (1982) 1471.
[25] C. Dimitropoulos, J. Pelzl, F. Borsa, Phys. Rev. B 41 (1990) 3914.
[26] N. Bloembergen, E.M. Purcell, R.V. Pound, Phys. Rev. 73 (1948) 679.
[27] G. Eckold, H. Grimm, M. Stein-Arsic, Physica B 180 & 181 (1992) 336.
[28] C. Odin, Magn. Reson. Chem. 42 (2004) 381.